Molecular Crystals and Liquid Crystals
Publication details, including instructions for authors and subscription information:
http://www.tandfonline.com/loi/gmcl20

Thermal Analysis of Supramolecular Hydrogen-Bonded Liquid Crystals Formed by Nonyloxy and Alkyl Benzoic Acids

C. Kavitha [a], N. Pongali Sathya Prabu [a] & M. L. N. Madhu Mohan [a]
[a] Liquid Crystal Research Laboratory (LCRL), Bannari Amman Institute of Technology, Sathyamangalam, India
Published online: 02 Apr 2013.

To cite this article: C. Kavitha, N. Pongali Sathya Prabu & M. L. N. Madhu Mohan (2013) Thermal Analysis of Supramolecular Hydrogen-Bonded Liquid Crystals Formed by Nonyloxy and Alkyl Benzoic Acids, Molecular Crystals and Liquid Crystals, 574:1, 96-113, DOI: 10.1080/15421406.2012.762500

To link to this article: http://dx.doi.org/10.1080/15421406.2012.762500

Mol. Cryst. Liq. Cryst., Vol. 574: pp. 96–113, 2013

ISSN: 1542-1406 print/1563-5287 online
DOI: 10.1080/15421406.2012.762500

Taylor & Francis
Taylor & Francis Group

Thermal Analysis of Supramolecular Hydrogen-Bonded Liquid Crystals Formed by Nonyloxy and Alkyl Benzoic Acids

C. KAVITHA, N. PONGALI SATHYA PRABU, AND M. L. N. MADHU MOHAN*

Liquid Crystal Research Laboratory (LCRL), Bannari Amman Institute of Technology, Sathyamangalam, India

A novel series of supramolecular hydrogen-bonded complexes (supramolecular hydrogen-bonded liquid crystal, SMHBLC) has been isolated from equimolar ratios of p-n-nonyloxy benzoic acid (9BAO) and seven p-n-alkyl benzoic acids (nBA) whose carbon number varied from ethyl to octyl. Complementary hydrogen bonds are formed between them. They have been investigated by polarizing optical microscopy (POM), differential scanning calorimetry (DSC) and further these data are utilized for the construction of phase diagram. Characteristic textures of the orthogonal and tilted phases have been recorded and compared. A new smectic ordering referred to as smectic X is characterized by various techniques. Odd–even effects are evinced in transition temperatures. The order of the transitions is distinguished by thermal analysis. The magnitude of experimental optical tilt angle in smectic C of all the homologs is fitted to a power law and the value of exponent is found to concur with the mean field theory predicted value.

Keywords Hydrogen-bonded liquid crystals; odd–even effect; optical tilt angle; smectic X; thermal analysis

1. Introduction

In liquid crystals, hydrogen bond is an important driving force for engineering directional elements into supramolecular assemblies of noncovalently connected molecules [1,2]. The earliest example of the unique geometrical ramification of hydrogen bonding in supramolecular organization is the work of Bradfield and Jones [3], who, started some 70 years ago, showed that certain hydrogen-bonded dimmers of organic acids exhibit liquid crystallinity in their melts. Aromatic acid derivatives with alkoxy and alkyl terminal groups are known to show mesomorphism due to the dimerization of their carboxylic acid groups through hydrogen bonding [3] and this mesomorphism results from the proper combination of molecular interactions and the shape of molecules. Interest and curiosity in the relationship between hydrogen bond formation and mesomorphism have been exploited in the last decade by Paleos [4], Kato and Frechet [5], and Kato et al. [6]. An archetypal example is

*Address correspondence to M. L. N. Madhu Mohan, Liquid Crystal Research Laboratory (LCRL), Bannari Amman Institute of Technology, Sathyamangalam 638401, India. Tel.: +91-9442437480; Fax: +91-4295-223-775. E-mail: mln.madhu@gmail.com

their work on hydrogen bonding between aromatic acids and 4-substituted pyridyl group to stabilize low molar mass mesophases in binary mixtures, mixtures with polymeric components [5,6], and in chiral, mesomorphic networks comprising nonmesogenic precursors [7]. In view of the fact that Kato et al. prepared new liquid crystals induced by intermolecular hydrogen bonding between pyridyl moieties and carboxylic acid groups that are proton acceptors and proton donors, respectively [5,6], many new liquid crystals such as molecular liquid crystals [8,9], polymer liquid crystals [10,11], ferroelectric liquid crystals [12–14], room-temperature liquid crystals [15] have been prepared by using this method, because of the stability of intermolecular hydrogen bonding [14,16] and the synthetic directionality [13,15]. Thus, hydrogen bonding is one of the key interactions for chemical and biological processes in nature and also plays an important role in molecular aggregates for the association of molecules. Dipole–dipole interactions have long been taken into consideration in the design of liquid crystalline molecules [17,18]. In contrast, and with few exceptions, intermolecular hydrogen bonds that are stronger than dipole–dipole interactions had been considered to be deleterious for thermotropic liquid crystallinity in the past, because in many cases they cause molecular associations that raise melting temperatures or destroy molecular order of the mesophases, but recently [8,12,19–25] a number of supramolecular mesogenic materials have been obtained by molecular self-assembly through intermolecular hydrogen bonding. To explore the potential use of the hydrogen-bonded liquid crystals, mesogens consisting of only two aromatic rings have been designed to induce room-temperature mesophases [26]. Most of the published work up to early 1995 is summarized in two review papers, one, treating the subject in a general manner [20] and the other focusing specifically on carbohydrates [27]. Examples of more recent publications are quoted in Refs. [15,19,28–31].

The central theme of the present work is to study the physical and chemical properties of supramolecular hydrogen-bonded liquid crystals (SMHBLCs) formed by the blend of various combinations of alkyl and alkoxy carboxylic acids through intermolecular hydrogen bonds. Through our previous experience [32–42] in designing, synthesizing, and characterizing liquid crystals and in persistence of our efforts to understand the effect of hydrogen bonds, eight such homologous series designated as *m*OØ*n* (*m*BAO + *n*BA, where *n* varied from ethyl to octyl while *m* varied from pentyl to dodecyl) can be deduced with changing the alkyl and alkoxy carbon number. A systematic study of 12OØ*n* (12BAO + *n*BA), 11OØ*n* (11BAO + *n*BA), and 10OØ*n* (10BAO + *n*BA) homologous series has been carried out by the authors [43]. In the present work, design, synthesis, and characterization of seven 9OØ*n* (9BAO + *n*BA) homologs are discussed.

2. Experimental

Observations of optical textures are made with a Nikon polarizing microscope (Nikon, Tokyo, Japan) equipped with Nikon digital CCD camera system with 5 mega pixels and 2560 × 1920 pixel resolutions. The liquid crystalline textures are analyzed and stored with the assist of ACT-2U imaging software system. The temperature control of the liquid crystal cell is equipped with HCS402-STC 200 temperature controller (Instec, Boulder, CO) to a temperature resolution of $\pm 0.1^{\circ}$C. This unit is interfaced to a computer by IEEE – STC 200 to control and monitor the temperature. The liquid crystal sample, in its isotropic state is filled by capillary action into a commercially available polyamide 4-μm buffed cell (Instec). Optical extinction technique [38] is used for the determination of tilt angle in smectic C phase. Transition temperatures and corresponding enthalpy values are obtained

by differential scanning calorimetry (DSC; Shimadzu DSC-60, Japan). Fourier transform infrared (FTIR) spectra are recorded (ABB FTIR MB3000) and analyzed with the MB3000 software. The *p-n*-nonyloxy benzoic acid (9BAO) and *p-n*-alkyl benzoic acids (*n*BA, where *n* varied from ethyl to octyl) are supplied by Sigma-Aldrich (Munich, Germany), and all the solvents used are of high performance liquid chromatography (HPLC) grade.

2.1 Synthesis of SMHBLC

SMHBLC complexes examined in the present study are obtained by mixing 1:1 molar ratio of nonyloxy benzoic acid with various alkyl benzoic acids separately in DMF and reprecipitating after the evaporation as described in the reported literature [5,6]. Synthesis scheme of the present homologous series (9OØ*n*) of nonyloxy benzoic acid (9BAO) with *p-n*-alkyl benzoic acids (*n*BA, where *n* represents the alkyl carbon number and *n* varied from ethyl to octyl) is depicted in scheme along with the proposed molecular structure of 9OØ*n* in Fig. 1.

3. Results and Discussion

SMHBLCs isolated under the present investigation are white crystalline solids and stable at room temperature (∼30°C). They are insoluble in water and sparingly soluble in common organic solvents such as methanol, ethanol, benzene, and dichloro methane. However, a high degree of solubility is found in coordinating solvents such as dimethyl sulfoxide (DMSO), dimethyl formamide (DMF), and pyridine. All these mesogens melt at specific temperatures below 76.7°C (Table 1). They show high thermal and chemical stability when subjected to repeated thermal scans performed during polarizing optical microscopy (POM) and DSC studies.

3.1 Phase Identification

The observed phase variance, transition temperatures, and corresponding enthalpy values obtained by DSC in the cooling and heating cycles for the 9OØ*n* complexes are presented in Table 1. It is found that these data are in concurrence with POM data. The mesogens of the nonyloxy benzoic acid (9BAO) with various *p-n*-alkyl benzoic acids (*n*BA, where *n* varied from ethyl to octyl) designated as 9OØ*n* homologous series are found to exhibit characteristic phases [18], viz., nematic (N; schlieren brushes, Plate 1), smectic C (schlieren texture, Plate 2), and smectic F (mosaic-schlieren, Plate 3, i.e., mosaic platelets separated by very fine lines containing schlieren-like brushes, but does not show actual intersections in the form of crosses). A new phase, smectic X (worm-like texture, Plate 4), has been identified in this complex. As previously mentioned, a systematic study of 12OØ*n*, 11OØ*n*, and 10OØ*n* homologous series has been carried out [43] in which smectic X phase has been identified and characterized. The textural morphology and the thermal characteristics of the smectic X phase observed in the present study exactly resemble the reported [43] data.

A brief description of schlieren brushes of nematic phase is detailed below; Plate 1 specifies nematic phase encompassing point singularity with four brushes. These brushes meet at point singularities on the surface of the preparation or point singularities are the origins of the brushes. The black bands or schlieren occurring throughout the texture are the regions of extinction and are often referred to as schlieren brushes [18]. The point

Table 1. Transition temperatures and enthalpy values obtained by various techniques for 9OØ*n* homologous series

Complexes	Phase variance	Technique	Melt	N	C	X	F	Crystal
9OØ8	NCXF	DSC(h)	74.1 (26.46)	126.3 (0.56)	112.1 (0.66)	84.2 (0.48)	84.7 (0.32)	
		DSC(c)		121.4 (1.41)	108.1 (0.83)	83.1 (1.96)	[b]	69.9 (23.39)
		POM(c)		122.3	108.7	83.4	83.8	70.1
9OØ7	NCF	DSC(h)	63.2 (24.69)	128.9 (2.94)	110.7 (1.28)		72.9 (1.06)	
		DSC(c)		126.7 (3.77)	108.3 (0.66)		70.9 (1.50)	58.8 (22.72)
		POM(c)		127.5	108.8		71.3	59.0
9OØ6	NCXF	DSC(h)	54.3 (19.68)	126.8 (0.51)	108.9 (0.30)	[a]	[a]	
		DSC(c)		121.7 (0.67)	[a]	55.1 (0.36)	55.6 (0.52)	51.2 (17.87)
		POM(c)		122.8	110.8	55.6	55.8	51.3
9OØ5	NC	DSC(h)	57.9 (26.26)	133.2 (1.01)	121.9 (0.27)			
		DSC(c)		130.9 (2.88)	[a]			51.5 (23.57)
		POM(c)		131.3	119.9			51.8
9OØ4	NC	DSC(h)	60.7 (30.02)	127.1 (1.31)	105.3 (1.55)			
		DSC(c)		125.0 (3.30)	104.7 (0.74)			50.9 (27.19)
		POM(c)		125.8	105.4			51.2
9OØ3	NC	DSC(h)	76.7 (42.41)	130.6 (2.46)	112.3 (1.07)			
		DSC(c)		128.2 (2.79)	109.1 (0.58)			69.1 (40.72)
		POM(c)		129.1	109.7			69.5
9OØ2	NC	DSC(h)	66.5 (35.88)	123.7 (0.35)	73.5 (0.13)			
		DSC(c)		120.4 (1.96)	[a]			59.9 (33.45)
		POM(c)		121.2	72.6			60.2

Note. Temperatures (°C), enthalpy ($J \cdot g^{-1}$) are given in parentheses. h, Heating run; c, cooling run.
[a]Monotropic transition.
[b]Merged with crystal.

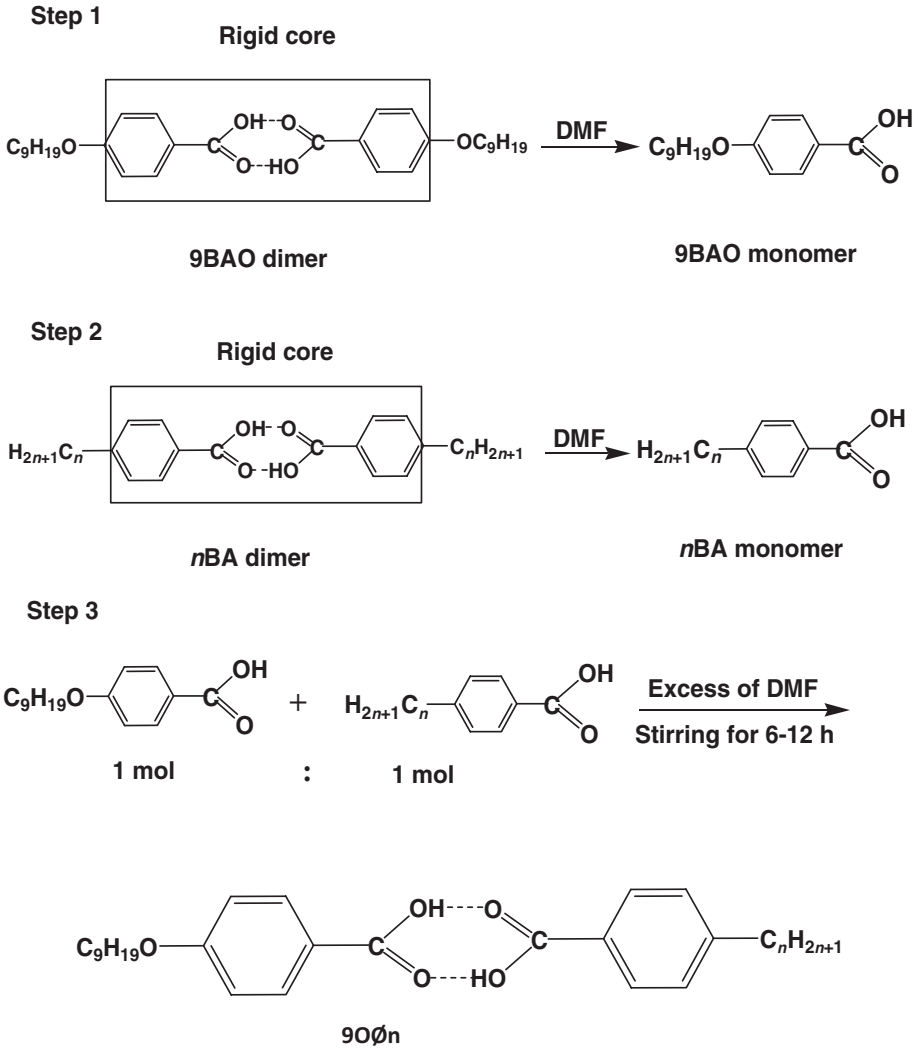

Figure 1. Synthesis scheme representing the formation of 9O*Øn* hydrogen-bonded series and the molecular structure of 9O*Øn* homologous series.

singularities are characterized by

$$|S| = \text{number of brushes}/4 = 4/4 = 1$$

With a positive sign when the brushes rotate in the same direction as that in which the polarizer and analyzer are simultaneously rotated in the crossed position and with a negative sign they turn in the opposite sense. In general, singularities with $S = +1/2, -1/2, +1, -1$ are known for nematics, but for the smectic C phase, all the point singularities are of the $S = \pm 1$ type. Therefore, $S = +1$ value calculated for the present texture revealed that the given Plate 1 is identical with that of a nematic phase with a texture enclosing schlieren four brushes.

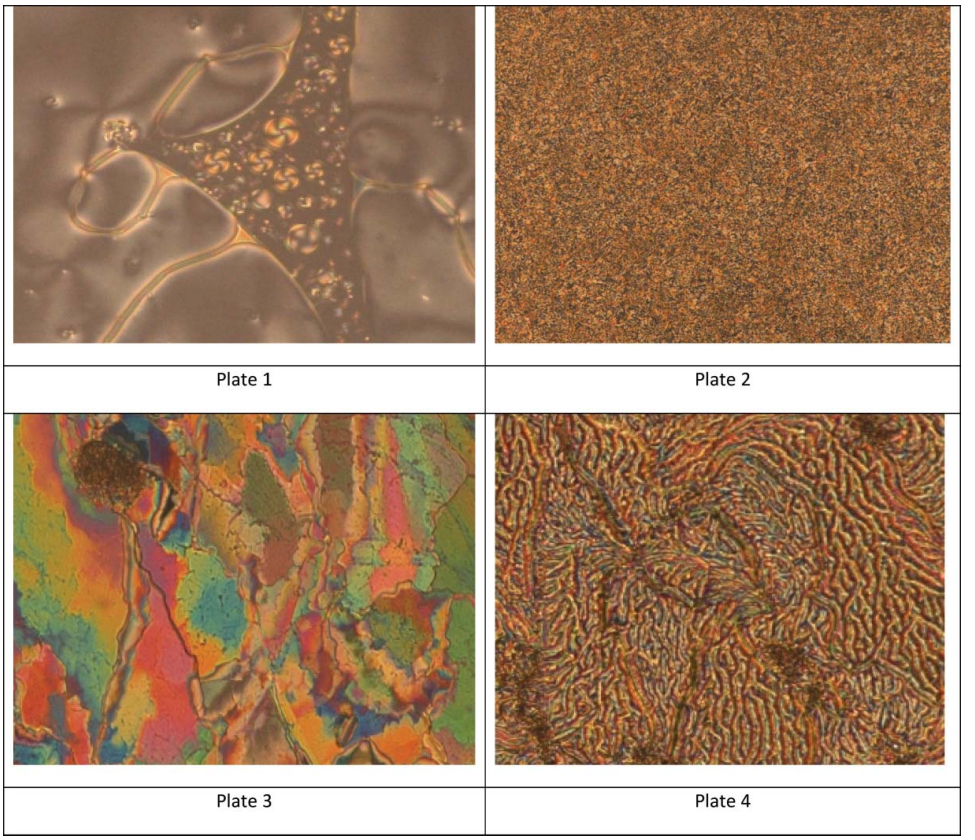

Plates 1–4. (1)Schlieren brush texture of nematic phase. (2)Schlieren texture of smectic C phase. (3) Mosaic-schlieren texture of smectic F phase. (4)Fully grown finger print worm-like texture of smectic X phase

The general phase sequence of various homologs of 9O*Øn* series in cooling and heating run of POM and DSC can be shown as

Iso. $\rightarrow$ N $\rightleftharpoons$ Sm C $\rightleftharpoons$ Sm X $\rightleftharpoons$ Sm F $\rightleftharpoons$ Crystal	(9OØ8)
Iso. $\rightleftharpoons$ N $\rightleftharpoons$ Sm C $\rightleftharpoons$ Sm F $\rightleftharpoons$ Crystal	(9OØ7)
Iso. $\rightleftharpoons$ N $\rightleftharpoons$ Sm C $\rightarrow$ Sm X $\rightarrow$ Sm F $\rightleftharpoons$ Crystal	(9OØ6)
Iso. $\rightleftharpoons$ N $\rightleftharpoons$ Sm C $\rightleftharpoons$ Crystal	(9OØ5, 9OØ4, 9OØ3)
Iso. $\rightleftharpoons$ N $\rightarrow$ Sm C $\rightleftharpoons$ Crystal	(9OØ2)

Monotropic and enantiotropic transitions are depicted as single and double arrows, respectively. The 9O*Øn* series exhibits new phase sequence compared to their precursors (9BAO and *n*BA) and is clearly evident from Table 2.

Table 2. Phase variance exhibited by 9OØ*n* series and their precursors

9OØ*n* series		BAO		9OØO*n* series		*n*BA series	
Hydrogen-bonded complex	Phase variance	Precursor	Phase variance	Hydrogen-bonded complex	Phase variance	Precursor	Phase variance
9OØ8	NCXF	9BAO	NC	9OØO5	NC	8BA	NG
9OØ7	NCF			9OØO6	NCF	7BA	NG
9OØ6	NCXF			9OØO7	NCF	6BA	NG
9OØ5	NC			9OØO8	NCF	5BA	NG
9OØ4	NC			9OØO10	NCF	4BA	NG
9OØ3	NC			9OØO11	NCF	3BA	G
9OØ2	NC			9OØO12	NXC	2BA	G

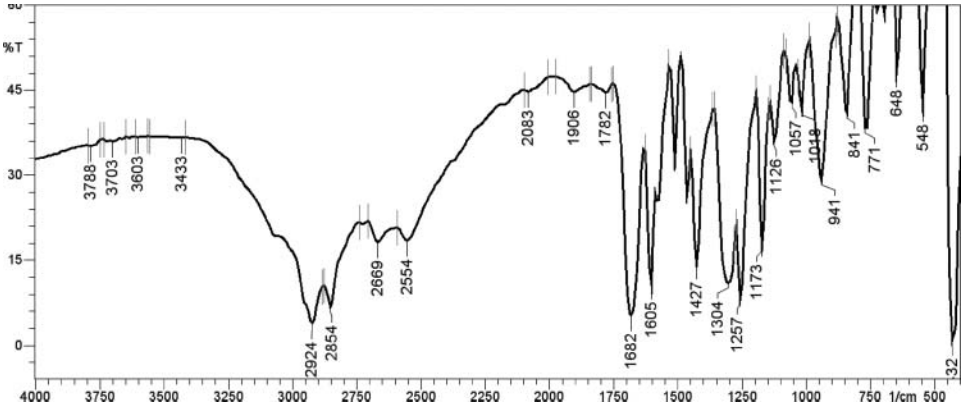

Figure 2. FTIR spectra of 9OØ6 complex

3.2 Spectroscopic Studies

3.2.1 Fourier Transform Infrared Spectroscopy (FTIR). At room temperature, FTIR spectra of all the SMHBLCs are recorded in the solid state (KBr). As a representative case, the FTIR spectrum of 9OØ6 is illustrated in Fig. 2. In the alkyloxy benzoic acids, carboxylic acid exists in monomeric form and the stretching vibration of C=O is observed at 1674 cm^{-1}. Further it is reported [44] that when a hydrogen bond is formed between carboxylic acids, it results in lowering of the carbonyl frequency, which has been detected in the present hydrogen-bonded complexes. A noteworthy feature in the spectrum of the 9OØ6 is the appearance of a sharp peak at 1682 cm^{-1}, which clearly suggests the dimmer formation, in particular the carbonyl group vibration [44–47]. A carboxylic acid existing in a monomeric form in dilute solution absorbs at about 1760 cm^{-1} because of the electron withdrawing effect. However, acids in concentrated solution or in solid state tend to dimerize through hydrogen bonding. It is reported [24] that this dimerization weakens the C=O bond and lowers the stretching force constant K, resulting in lowering of the carbonyl frequency of saturated acids to $\sim$1682 cm^{-1} (Table 3). Hence in the present complexes, the formation of hydrogen bonding is established by FTIR peak assignments. A similar trend of result is followed in all the other homologs.

Table 3. FTIR stretching frequencies of the 9OØ*n* complexes and their precursors

Complex (9OØ*n*)			Precursor (*n*BA)			Precursor (9BAO)	
9OØ*n*	$(CO)_{acid}$	$(OH)_{acid}$	*n*BA	$(CO)_{acid}$	$(OH)_{acid}$	$(CO)_{acid}$	$(OH)_{acid}$
9OØ8	1682	2924	8BA	1682	2924	1674	2924
9OØ7	1682	2924	7BA	1692	2927		
9OØ6	1682	2924	6BA	1687	2927		
9OØ5	1682	2924	5BA	1686	2927		
9OØ4	1682	2924	4BA	1686	2927		
9OØ3	1690	2924	3BA	1681	2959		
9OØ2	1682	2924	2BA	1687	2962		

3.3 DSC Studies

DSC thermograms of all the seven SMHBLCs are recorded in heating and cooling cycle. The accurately weighed individual sample is crimped in aluminum pan and loaded into the heating chamber. The instrument is programed to heat the sample with a predetermined scan rate ($5^{\circ}C{\cdot}min^{-1}$ and $10^{\circ}C{\cdot}min^{-1}$) and held at its respective isotropic temperature for 2 min so as to attain thermal stability. Nitrogen gas is continuously purged inside the heating chamber. Cooling run is programed with identical scan rate ($5^{\circ}C{\cdot}min^{-1}$ and $10^{\circ}C{\cdot}min^{-1}$). The respective resultant equilibrium transition temperatures and corresponding enthalpy values of the mesogens of the homologous series are listed separately in Table 1. POM studies also concur with the DSC transition temperatures. As a representative case, DSC thermogram in both the heating and cooling cycles of 9OØ7 is depicted in Fig. 3(a), which

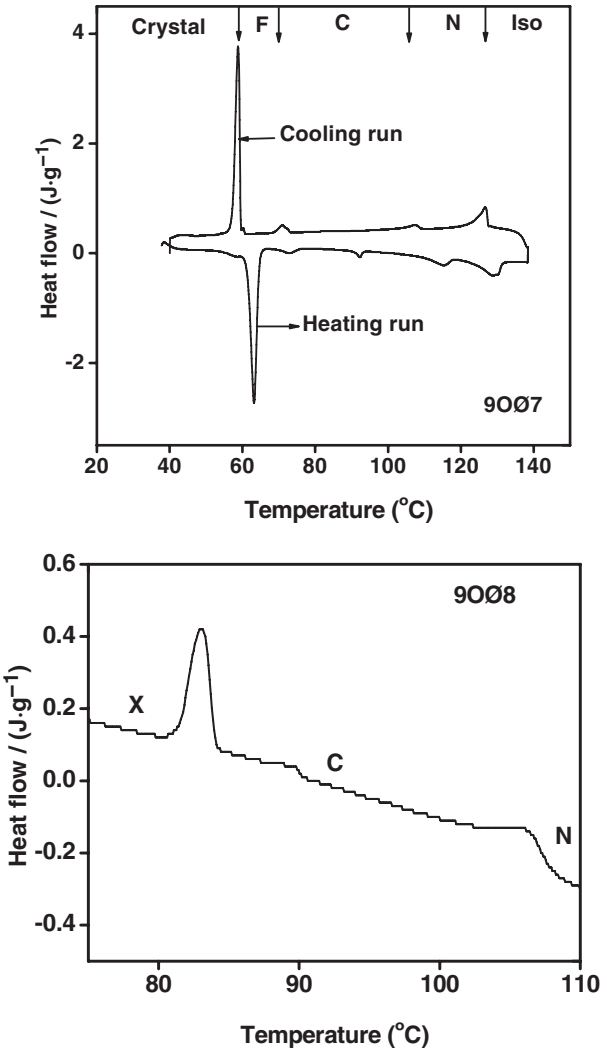

Figure 3. (a) DSC thermogram of 9OØ7 complex. (b) DSC thermogram of 9OØ8 complex depicting smectic X phase in cooling run.

Table 4. Sum of enthalpy values obtained in heating and cooling run

Hydrogen-bonded complexes	DSC cycles	
	Σ Enthalpy values of all transitions in heating cycle ($J \cdot g^{-1}$)	Σ Enthalpy values of all transitions in cooling cycle ($J \cdot g^{-1}$)
9OØ8	28.16	27.59
9OØ7	29.97	28.65
9OØ6	20.19	18.54
9OØ5	27.27	26.45
9OØ4	32.88	31.23
9OØ3	45.94	44.09
9OØ2	36.23	35.41

shows various mesogenic transitions. In addition, the well-resolved phase transitions of sample 9OØ8, corresponding to isotropic to nematic, nematic to smectic C, and smectic C to smectic X in the cooling cycle are also depicted in Fig. 3(b).

3.3.1 Thermal Equilibrium Exhibited by the Complexes. According to principles of thermodynamics, the energy involved in the endothermic (heating) process and exothermic (cooling) process should be exactly equal. In other words, for a thermally stable mesogen, the total heat absorbed in the endothermic process should be equal to the sum of heats evolved during the exothermic process. From the thorough observation of the DSC thermograms of the Entire 9O*Øn* series, it is not surprising to note that the sum of enthalpy values obtained by the complexes both in the heating and cooling runs, for the various phase transitions, i.e., from isotropic to nematic, nematic to smectic C, smectic C to smectic X, smectic X to smectic F, and smectic F to crystal, are found to be almost identical. Table 4 confirms the above statement and verifies the principles of thermodynamics. The total enthalpy value obtained in both heating and cooling run is found to follow a typical order, which is clearly portrayed in Fig. 4. The magnitudes of total enthalpy values for both the heating and the cooling cycles are closely following one another with the former having slightly higher value than that of the later one. This is an interesting observation that is detected in the present SMHBLC series.

3.3.2 Thermal Analysis. Landau theory and mean field theory [48] are the theories that discuss the phase transitions in liquid crystalline substance. Two theories on the whole can be summarized as physical systems in which phase transition can occur is usually characterized by one or more long range order parameters. A phase transition can be accompanied either by a continuous change or by a discontinuous change in the equilibrium value of the order parameter when the system transforms from one phase to the other. It is said to be the first-order transition when it is discontinuous, and if the state is continuous, it is assigned to be second-order transition. Thus, the theoretical description of a phase transition is equivalent to the determination of the free-energy density as a function of the order parameter, its spatial derivatives, and the temperature. Determination of phase transition order by experimental technique carried out by Navard and Cox [49] supplements the above-mentioned arguments.

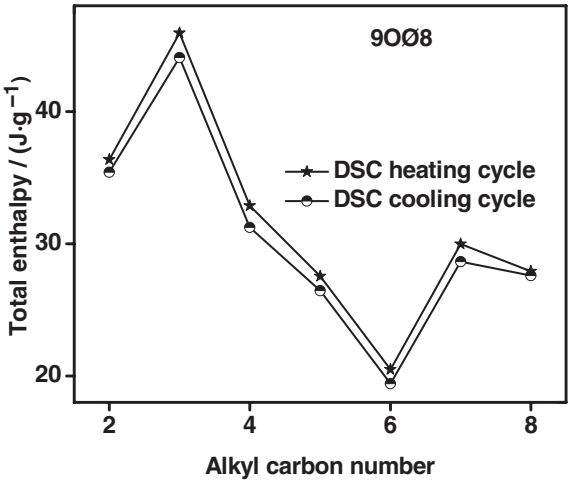

Figure 4. Total enthalpy values obtained in heating and cooling run of DSC thermograms of entire 9O*Øn* complexes.

Navard and Cox [49] utilized thermal analysis for the differentiation of first- and second-order transitions of liquid crystal complexes based on DSC thermograms. The DSC scanning rate or the weight of the sample measured can be varied for this purpose, but for the accurate results and convenience, the former is preferred in the present study. Transition peaks obtained by DSC studies at two scan rates, one being twice the other, are measured and their ratio (Cox parameter, N_C) is employed for this purpose. The first- and the second-order transitions can be classified based on the ratio (N_C) of the measured heights, $1 < N_C \geq \sqrt{2}$ for an isothermal first-order transition and $N_C = 2$ for a second-order transition.

For all the homologs, DSC thermograms at 5°C·min^{-1} and 10°C·min^{-1} are obtained and as a representative case, the thermal analysis of 9OØ8 complex is discussed. The DSC thermograms of the sample 9OØ8 at 5°C·min^{-1} and 10°C·min^{-1} scan rates are represented in Fig. 5. The magnitude of the corresponding peaks, the phase segregations along with the cooling run at 5°C·min^{-1} (a) and 10°C·min^{-1} (b) scan rates are depicted in Fig. 5. The values of N_C for the isotropic to nematic, nematic to smectic C, and smectic C to smectic X transitions for 9OØ8 complex are presented in Table 5. From this qualitative analysis, the values of N_C are calculated and found to be 1.70 for isotropic to nematic transition,

Table 5. Comparison of DSC peak heights along with N_C values across various transitions in 9OØ8 complex

		Peak height		
Complex	DSC	Nematic	Sm C	Sm X
9OØ8	5°C·min^{-1}	0.34 mW	0.04 mW	0.21 mW
	10°C·min^{-1}	0.58 mW	0.07 mW	0.37 mW
Ratio (N_C)	(10°C·min^{-1})/(5°C·min^{-1})	1.70	1.75	1.76

Note. Sm, smectic.

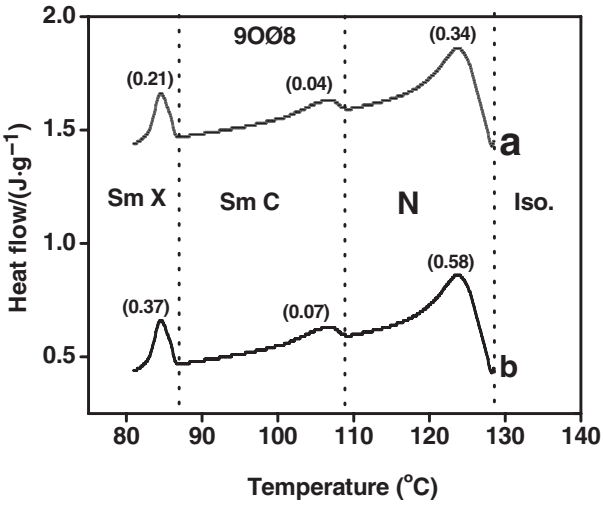

Figure 5. DSC thermograms of 9OØ8 complex performed at two different scan rates. Thermogram (a) and (b) represents scan rates of $5^{\circ}C{\cdot}min^{-1}$ and $10^{\circ}C{\cdot}min^{-1}$, respectively

1.75 for nematic to smectic C transition, and 1.76 for smectic C to smectic X transition. Thus, N_C is found to be below 2 indicating that all these transitions are of first order. Quantitatively, the higher value of enthalpy obtained in DSC studies (Table 1) also serves as an additional evidence for its first-order transition. Further, from the enthalpy values based on the above-mentioned procedures, we can classify smectic C to smectic X as weak first-order transition.

3.4 Phase Diagram of Precursors

Phase diagrams of precursors 9BAO and *n*BAs are composed of nematic, smectic C, and nematic, smectic G, respectively (Table 2).

3.4.1 Phase Diagram of 9OØn. Phase diagram of nonyloxy benzoic acid and *p-n*-alkyl benzoic acids homologous series (9OØ*n*) are depicted in Fig. 6. Following points can be elucidated from Fig. 6:

(a) The 9OØ*n* hydrogen-bonded homologous series exhibits nematic as orthogonal phase and smectic C, smectic X, and smectic F as tilted phases.
(b) Compared to the precursors, in the present SMHBLCs two smectic phases namely smectic X and smectic F is induced while smectic G phase is completely annihilated.
(c) Smectic X phase is induced only in octyl benzoic acid and hexyl benzoic acid, quenching the thermal range of smectic C. Further smectic X is sandwiched between smectic C and smectic F phases.
(d) The thermal span of nematic phase is observed to be invariant with increasing alkyl chain length.
(e) An interesting observation is the presence of odd–even effects at isotropic to nematic and nematic to smectic C transition temperatures.

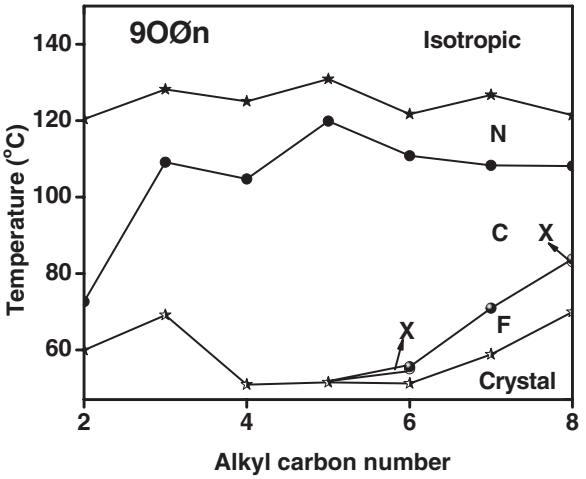

Figure 6. Phase diagram of 9O*Øn* homologous series.

(f) A gradual decrease in the crystallization temperatures is observed from octyl benzoic acid to butyl benzoic acid.
(g) The occurrence of smectic X phase is attributed to the *l*/*d* ratio of the homologous series. The lower homologs failed to posses the threshold value of *l*/*d* ratio, which in turn reflects in the absence of smectic X phase.

3.4.2 Odd–Even Effect. The origin of the odd–even effect [48,50,51] can be understood from the consideration of the molecular structure of 9O*Øn*. In the even numbers of the series, the disposition of the end group is to enhance the molecular anisotropy and hence molecular order, whereas in the odd number it has the opposite effect. As the chain length increase, their flexibility increases and the odd–even effect observed in the present series is in accordance with the quantitative calculations proposed by Marcelja [50].

From Fig. 7(a) and (b), it can be observed that the magnitudes of the isotropic to nematic and nematic to smectic C transition temperatures corresponding to the homologous with even carbon number (9OØ2, 9OØ4, 9OØ6, and 9OØ8) exhibit one type of behavior, while the odd counter parts (9OØ3, 9OØ5, and 9OØ7) show a different increment and is known as odd–even effect.

Considering flexibility due to end chains, Mercelja [50] incorporated the configurational statistics of the end chains in the theory of the nematic phase in a Flory-type calculation [52]. In addition to conformational energy, each C–C bond in the end chain is subjected to a mean field, which depends both on the orientational order of the rigid central part and that of the end chain. A high probability of occurrence of the all trans-configuration for short chains is considered for the strong odd–even effect for lower homologous. The increase in conformational flexibility for the higher homologs is seen as an extension of this effect.

Luckhurst [53] refined the calculations made by Pink model, which shows that while the odd–even effect in transition temperature can be understood as a consequence of the odd–even effect in the chain-order parameter with respect to the molecular axis, the odd–even effect in the rigid segment-order parameter is the consequence of at least such

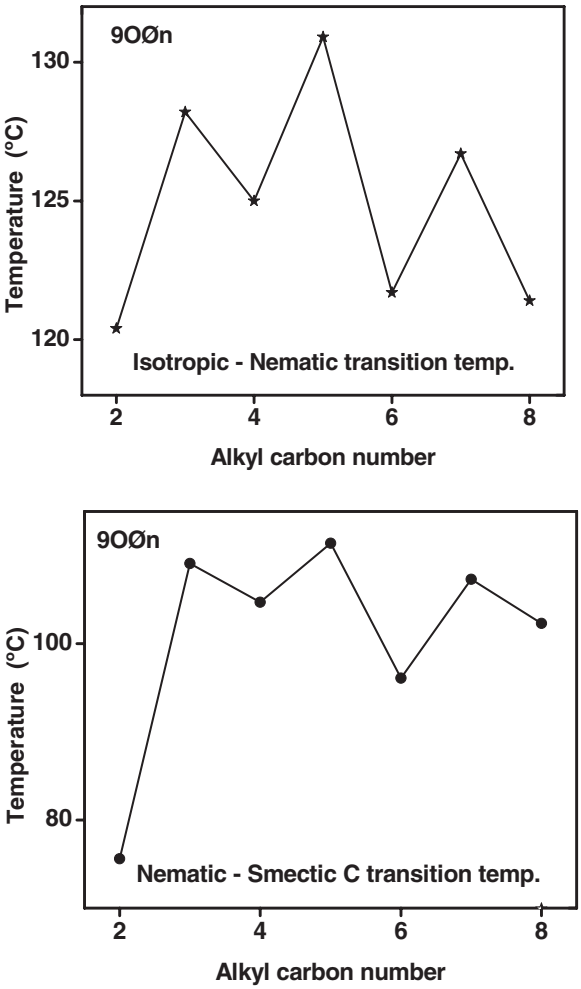

Figure 7. (a) Odd–even effect across isotropic to nematic transition temperatures in 9O*Øn* series. (b) Odd–even effect across nematic to smectic C transition temperatures in 9O*Øn* series.

an effect in the mean-square deviation and used to make successful calculations for compounds that have two rigid cyano biphenyl moieties linked by flexible spacers, in which the odd–even alteration in transition temperature is very strong. In compounds with alkyl and alkoxy end chains, it is already known [43] that the isotropic to nematic transition temperatures show odd–even effects. In addition to this odd–even effect, at the interface of nematic to smectic C transition temperature is also noticed. For short alkyl chain lengths, this alteration effect is more pronounced, whereas it becomes less marked with longer alkyl chain lengths. Odd carbon atom alkyl chain (3BA, 5BA, and 7BA) having a terminal CH_3, extends along the molecular axis increasing the transition temperature, whereas in an even number carbon chain (2BA, 4BA, 6BA, and 8BA), the terminal chain lies off the molecular axis decreasing the transition temperature, which may be the appropriate explanation for the occurrence of this effect. The entropy of melting increases with flexible chains, which serves to lower the melting point and to augment the liquid crystalline range.

4. Occurrence of Smectic C and Measurement of Optical Tilt Angle

Smectic C phase is the first classified phase in which the molecular long axes of the constituent molecules were found to be tilted with respect to the normal of the layer planes. A large number of experimental studies are there concerning the effect of small changes in the molecular structure on the incidence and temperature dependence of the smectic C phase. The occurrence and abundance of high thermal span of smectic C in the present SMHBLC can be justified by the molecular structure that is supplemented by the following arguments:

a. Molecules having two terminal alky chains especially alkyl/alkoxy groups exhibit smectic C phase predominantly.
b. Approximately, symmetrical molecular structure of the mesogens usually favors smectic C phase.
c. The molecular structure of the constituent molecules, particularly the length of the chains of the terminal alkyl or alkoxy groups, influences the occurrence of smectic C phase.

The variation of tilt angle $\theta(T)$ with temperature, reflecting the growth of order parameter in smectic C phase is measured by optical extinction method [38] in all the homologs of 9OØ*n* series. The tilt angle is found to increase with decreasing temperature. It is observed from the Fig. 8 that $\theta(T)$ attains a characteristic maximum value. It can be observed from Fig. 8 that the magnitude of tilt angle increases with the increment in the alkyl chain. The large magnitudes of the tilt angle in higher homologs are attributed to the enhanced orientational disorder introduced by the lengthy flexible part of the molecule. Hence, higher homologs with extended flexible part in SMHBLCs are argued to contribute positively to the inclined [23] soft covalent hydrogen bonding interaction for the realization of tilted phases of applicational interest.

The observed temperature variation of $\theta(T)$ appears to follow a power law relationship given by

$$\theta(T)\alpha(T_C - T)^{\beta}, \tag{1}$$

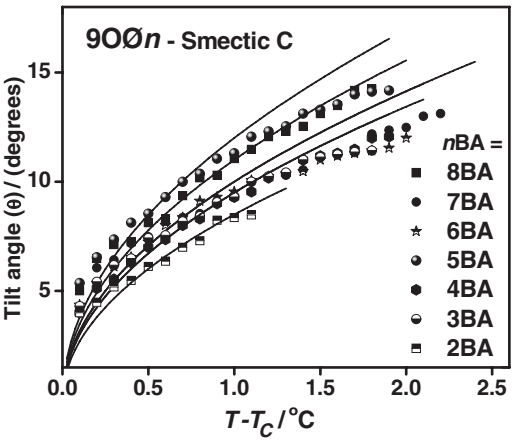

Figure 8. Temperature variation of tilt angle in smectic C phase of 9OØ*n* complexes (*n* varied from ethyl to octyl carbon number). Solid lines indicate the fit deduced from mean field theory.

where T_C represents the transition temperature, β the critical exponent component value, and T is the temperature at which $\theta(T)$ is experimentally determined.

The data of $\theta(T)$ for the members of 9OØ*n* in smectic C phase are fitted (Fig. 8) to Eq. (1) to study the growth of order parameter in smectic C phase. The critical exponent β value estimated by fitting the data of $\theta(T)$ to Eq. (1) is found to be 0.50 to agree with the mean field predicted value [48,54] to infer the long-range interaction of transverse dipole moment for the stabilization of the tilted smectic C phase.

5. Characterization of Smectic X Phase

Smectic X phase, which has been identified in two complexes namely 9OØ8 and 9OØ6, is characterized by textural studies. Furthermore, the observed smectic X phase in the present study exactly resembles the smectic X reported in our previous study [43].

In both the above complexes, smectic X is sandwiched between conventional smectic C and smectic F phases. This serves as one of the strongest evidence to identify this new phase, smectic X as smectic ordering.

5.1 Textural Study of Smectic X Phase

The hydrogen-bonded complexes 9OØ8 and 9OØ6 on cooling from isotropic phase forms nematic droplets with schlieren four brushes (Plate 1), on further cooling the mesogen nematic transforms into smectic C phase with schlieren texture (Plate 2). On additional cooling, the schlieren texture is transformed into a worm-like texture (Plate 4), which is designated as smectic X. The thermal width of this phase is observed to be very narrow ($<1^\circ$C) and the fully grown phase is shown in Plate 4. The striations in the worm-like texture are manifestation of the presence of helicoidal structure. With further decrement in temperature, this phase paves way for mosaic-schlieren texture of smectic F phase as shown in Plate 3. Interestingly, this smectic X phase is observed to be a monotropic transition.

5.2 DSC Studies of Smectic X Phase

Interestingly, the smectic X phase exhibits monotropic transition in the performed thermal scans and hence it is observed only in the cooling run of the 9OØ8 complex (Fig. 3(b)).

5.3 Ordering in Smectic X

Smectic X phase is sandwiched between conventional smectic C and smectic F phases. It is reported by us [43] that the molecular orientation in this phase is due to the flipping of the molecules. The high magnitude of the helix in smectic X phase, compared to its preceding and succeeding phases, stands as a token of evidence for the molecular reorientation. Thermodynamical conditions favor this smectic X phase with narrow thermal span, where the flipping of the molecules occur. POM, optical tilt angle, and helicoidal structural studies enable this phase to be a smectic ordering [43]. This argument is valid with evidence where, smectic X is sandwiched between two smectic orderings.

The ratio of length of the molecule (l) to the interlamellar distance (d) plays a pivotal role in the formation of various phases. If the layer spacing is equal to the molecular length, smectic phases are observed. However, if the layer spacing is smaller than the molecular length, the molecules undergo rapid restricted molecular motion forming higher order smectic phases. In very few cases, the molecules protrude into other smectic layers,

which are referred as interdigitated phases. Based on the preliminary textural and thermal data of 9OØ8 and 9OØ6, when the liquid crystal is cooled from smectic C, it is believed that interdigitations takes place leading to the formation of smectic X phase. On further cooling, the interdigitations ceases and higher order smectic F phase is formed.

6. Conclusions

Design and synthesis of liquid crystals with alkyl-nonyloxy terminal groups is carried out, which paved way for synthesis of many more similar hydrogen-bonded liquid crystals by varying the alkyl/alkyloxy terminal group. It is found that these liquid crystals exhibit rich phase polymorphism with orthogonal and tilted phases. The abundance of thermal width of smectic C is of interest along with the occurrence of new smectic ordering.

Acknowledgments

The divine blessings of almighty Bannari Amman, the infrastructural support rendered by Bannari Amman Institute of Technology, and the financial support rendered by the Board of Research in Nuclear Sciences (BRNS) of Department of Atomic Energy (DAE), India (sanction no. 2012/34/35/BRNS) are gratefully acknowledged by the authors.

References

[1] (a) Lehn, J. M. (1995). *Supramolecular Chemistry: Concepts and Perspectives*, A Personal Account Built Upon the George Fisher Baker Lectures in Chemistry at Cornell University: Rome, New York; (b) Wuest, J. D. (1995). *Mesomolecules: from Molecules to Materials*, Chapman and Hall: New York.
[2] Kumar, S. (2011). *Chemistry of Discotic Liquid Crystals*, CRC Press: Boca Raton, FL.
[3] Bradfield, A. E., & Jones, B. (1929). *J. Chem. Soc.*, 2660.
[4] Paleos, C. M., & Siourvas, D. T. (2001). *Liq. Cryst.*, *28*, 1127.
[5] Kato, T., & Frechet, J. M. J. (1989). *J. Am. Chem. Soc.*, *111*, 8533.
[6] Kato, T., Frechet, J. M. J., Wilson, P.G., Saito, T., Uryu, T., Fujishima, A., Jin, C., & Kaneuchi, F. (1993). *Chem. Mater.*, *5*, 1094.
[7] Kihara, H., Kato, T., Uryu, T., & Frechet, J. M. J. (1998). *Liq. Cryst.*, *24*, 413.
[8] Kato, T., Fujishima, A., & Frechet, J. M. J. (1990). *Chem. Lett.*, 919.
[9] Kato, T., Wilson, P. G., Fujishima, A., & Frechet, J. M. J. (1990). *Chem. Lett.*, *19*, 2003.
[10] Kato, T., & Frechet, J. M. J. (1989). *Macromolecules*, *22*, 3818.
[11] Kumar, U., Kato, T., & Frechet, J. M. J. (1992). *J. Am. Chem.*, *114*, 6630.
[12] Kumar, U., Frechet, J. M. J., Kato, T., Ujiie, S., & Iimura, K. (1992). *Angew. Chem. Int. Ed. Engl.*, *31*, 1531.
[13] Yu, L. J. (1993). *Liq. Cryst.*, *14*, 1303.
[14] Tian, Y. Q., Su, F. Y., Shao, Y. Y., Lu, X. Y., Tang, X. Y., Zhao, X. G., & Zhou, E. L. (1995). *Liq. Cryst.*, *19*, 743.
[15] Kato, T., Fukumasa, M., & Frechet, J. M. J. (1995). *Chem. Mater.*, *7*, 368.
[16] Kato, T., Uryu, T., Kanelechi, F., Jin, C., & Frechet, J. M. J. (1993). *Liq. Cryst.*, *14*, 1311.
[17] Gray, G. W. (1987). *Thermotropic Liquid Crystals*, Wiley Ed: Chichester.
[18] Gray, G. W., & Goodby, J. W. (1984). *Smectic Liquid Crystals*, Leonard Hill: Glasgow.
[19] Kato, T., & Frechet, J. M. J. (1995). *Macromol. Symp.*, *95*, 311.
[20] Paleos, C. M., & Tsiourvas, D. (1995). *Angew. Chem. Int. Ed. Engl.*, *34*, 1696.
[21] Lehn, J. M. (1993). *Makromol. Chem. Macromol. Symp.*, *69*, 1.
[22] Bruce, D. W., & Price, D. J. (1994). *Adv. Mater. Opt. Electron.*, *4*, 273.
[23] Sato, A., Kato, T., & Uryu, T. (1996). *J. Polym. Sci., Part A: Polym. Chem.*, *34*, 503.

[24] Kato, T., Kihara, H., Uryu, T., Fujishima, A., & Frechet, J. M. J. (1992). *Macromolecules*, *25*, 6836.
[25] Malik, S., Dhal, P. K., & Mashelkar, R. A. (1995). *Macromolecules*, *28*, 2159.
[26] Fukumasa, M., Kato, T., Uryu, T., & Frechet, J. M. J. (1993). *Chem. Lett.*, *22*, 65.
[27] Prade, H., Miethchen, R., & Vill, V. (1995). *J. Prakt. Chem.*, *337*, 427.
[28] Treybig, A., Dorscheid, C., Weissflog, W., & Kresse, H. (1995). *Mol. Cryst. Liq. Cryst.*, *260*, 369.
[29] Araki, K., Kato, T., Kumar, U., & Frechet, J. M. J. (1995). *Macromol. Rapid Commun.*, *16*, 733.
[30] Miethchen, R., Holz, J., Prade, H., & Liptak, A. (1992). *Tetrahedron*, *48*, 3061.
[31] Wilson, L. M. (1995). *Liq. Cryst.*, *18*, 381.
[32] Chitravel, T., Madhu Mohan, M. L. N., & Krishnakumar, V. (2008). *Mol. Cryst. Liq. Cryst.*, *493*, 17.
[33] Vijayakumar, V. N., & Madhu Mohan, M. L. N. (2010). *Solid State Sci.*, *12*, 482.
[34] Pongali Sathya Prabu, N., Vijayakumar, V. N., & Madhu Mohan, M. L. N. (2011). *Phys. B : Condens. Matter*, *406*, 1106.
[35] Vijayakumar, V. N., Murugadass, K., & Madhu Mohan, M. L. N. (2009). *Mol. Cryst. Liq. Cryst.*, *515*, 39.
[36] Vijayakumar, V. N., & Madhu Mohan, M. L. N. (2009). *Braz. J. Phys.*, *39*, 601.
[37] Pongali Sathya Prabu, N., Vijayakumar, V. N., & Madhu Mohan, M. L. N. (2011). *J. Mol. Struct.*, *994*, 387.
[38] Vijayakumar, V. N., & Madhu Mohan, M. L. N. (2009). *Solid State Commun.*, *149*, 2090.
[39] Madhu Mohan, M. L. N., Kumar, P. A., Goud, B. V. S., & Pisipati, V. G. K. M. (1999). *Mater. Res. Bull.*, *34*, 2167.
[40] Pongali Sathya Prabu, N., Vijayakumar, V. N., & Madhu Mohan, M. L. N. (2011). *Mol. Cryst. Liq. Cryst.*, *548*, 73.
[41] Kumar, P. A., Madhu Mohan, M. L. N., Potukuchi, D. M., & Pisipati, V. G. K. M. (1998). *Mol. Cryst. Liq. Cryst.*, *325*, 127.
[42] Madhu Mohan, M. L. N., Kumar, P. A., & Pisipati, V. G. K. M. (2001). *Mol. Cryst. Liq. Cryst.*, *366*, 431.
[43] (a) Kavitha, C., Pongali Sathya Prabu, N., & Madhu Mohan, M. L. N. (2012). *Phys. B: Condens. Matter*, *407*, 859; (b) Kavitha, C., Pongali Sathya Prabu, N., & Madhu Mohan, M. L. N. (2012). *Phase Trans.*, *85*, 973.
[44] Pavia, D. L., Lampman, G. M., & Kriz, G. S. (2007). *Introduction to Spectroscopy*, Thomson, Brooks/Cole: Belmont, CA.
[45] Nakamoto, K. (1978). *Infrared and Raman Spectra of Inorganic and Co-ordination Compounds*, Interscience: New York.
[46] Xu, J. (2006). *J. Mater. Chem.*, *16*, 3540.
[47] Frechet, J. M. J., & Kato, T. (1992). Patent US No. 5139696.
[48] (a) Chandrasekhar, S. (1977). *Liquid Crystals*, Cambridge University Press: New York; (b) Priestly, E. B., Wojtowicz, P. J., & Sheng, P. (1975). *Introduction to Liquid Crystals*, Plenum Press: New York.
[49] Navard, P., & Cox, R. (1984). *Mol. Cryst. Liq. Cryst.*, *102*, 261.
[50] (a) Mercelja, S. (1973). *Solid State Commun.*, *13*, 759; (b) Mercelja, S. (1974). *J. Chem. Phys.*, *60*, 3599.
[51] Senthil, S., Rameshbabu, K., & Wu, S. L. (2006). *J. Mol. Struct.*, *783*, 215.
[52] Flory, P. J. (1956). *Proc. Roy. Soc. London*, *A234*, 73.
[53] Luckhurst, G. R. (1986). Nematic Liquid Crystals formed from flexible molecules: a molecular field theory. In: L. L. Chapoyed (Ed.), *Recent Advances in Liquid Crystalline Polymers*, Elsevier: London, pp. 105–107.
[54] Stanley, H. E. (1971). *Introduction to Phase Transition and Critical Phenomena*, Clarendon Press: New York.